



1 **Concomitant ocean acidification and increasing total alkalinity at a coastal site in the NW**

2 **Mediterranean Sea (2007-2015)**

3

4 Lydia Kapsenberg<sup>1</sup>, Samir Alliouane<sup>1</sup>, Frédéric Gazeau<sup>1</sup>, Laure Mousseau<sup>1</sup>, and Jean-Pierre  
5 Gattuso<sup>1,2,§</sup>

6

7 <sup>1</sup>Sorbonne Universités, Université Pierre et Marie Curie-Paris 6, CNRS-INSU, Laboratoire  
8 d'Océanographie de Villefranche, 06230, Villefranche-sur-Mer, France

9 <sup>2</sup>Institute for Sustainable Development and International Relations, Sciences Po, 27 rue Saint  
10 Guillaume, F-75007 Paris, France

11

12 <sup>§</sup>Corresponding author

13 E-mail: gattuso@obs-vlfr.fr

14 Phone: +33 4 93 76 38 59



15 **Abstract.** Monitoring global ocean change is necessary in coastal zones due to their physical and  
16 biological complexity. Here, we document changes in coastal carbonate chemistry at the time-  
17 series station, Point B, in the NW Mediterranean Sea, from 2007 through 2015, at 1 and 50 m.  
18 The rate of surface ocean acidification ( $-0.0028 \pm 0.0003$  units  $\text{pH}_T \text{ yr}^{-1}$ ) was faster-than-  
19 expected based on atmospheric carbon dioxide forcing alone. Changes in carbonate chemistry  
20 were predominantly driven by an increase in total dissolved inorganic carbon ( $C_T$ ,  $+2.97 \pm 0.20$   
21  $\mu\text{mol kg}^{-1} \text{ yr}^{-1}$ ),  $> 50\%$  of which was buffered by a synchronous increase in total alkalinity ( $A_T$ ,  
22  $+2.08 \pm 0.19 \mu\text{mol kg}^{-1} \text{ yr}^{-1}$ ). The increase in  $A_T$  was unrelated to salinity and its cause remains to  
23 be identified. Interestingly, concurrent increases in  $A_T$  and  $C_T$  were most rapid from May to July.  
24 Changes at 50 m were slower compared to 1 m. It seems therefore likely that changes in coastal  
25  $A_T$  cycling via a shallow coastal process gave rise to these observations. This study exemplifies  
26 the importance of understanding coastal ocean acidification through localized biogeochemical  
27 cycling that extends beyond simple air-sea gas exchange dynamics, in order to make relevant  
28 predictions about future coastal ocean change and ecosystem function.

29

30 **Keywords** – global ocean change, ocean acidification, time-series, pH, alkalinity, dissolved  
31 inorganic carbon,  $\text{pCO}_2$ , Mediterranean Sea, near-shore



## 32 1. Introduction

33 Maintaining time-series of oceanographic data is essential for understanding  
34 anthropogenic change in the ocean (Tanhua et al., 2013). On land, fossil fuel burning, cement  
35 production and land use changes have contributed ~580 Gt carbon to the atmosphere during the  
36 period 1750-2013 (Le Quéré et al., 2015). An estimated 29 % of this anthropogenic carbon is  
37 absorbed by the ocean in the form of carbon dioxide (CO<sub>2</sub>; Le Quéré et al., 2015), and causing  
38 global changes to the ocean carbonate system. Absorption of CO<sub>2</sub> by seawater produces carbonic  
39 acid, which decreases seawater pH, and is of great concern for biological processes and marine  
40 ecosystems (Doney et al., 2009; Gattuso and Hansson, 2011; Pörtner et al., 2014). Since the  
41 preindustrial era, global mean ocean pH has declined by 0.1 (Rhein et al., 2013). Due to the  
42 declining trend of ocean pH with increasing anthropogenic CO<sub>2</sub>, the process is termed ‘ocean  
43 acidification’, but this expression represents a suite of chemical changes, including increases in  
44 total dissolved inorganic carbon (C<sub>T</sub>) and partial pressure of CO<sub>2</sub> (pCO<sub>2</sub>) and decrease in calcium  
45 carbonate saturation states (Ω, aragonite and calcite; Dickson, 2010). Rates of ocean  
46 acidification differ by region and range from -0.0013 units pH yr<sup>-1</sup> (South Pacific) to -0.0026  
47 units pH yr<sup>-1</sup> (Irminger Sea, North Atlantic) and are reviewed in Bates et al. (2014). Such time-  
48 series remain spatially limited, especially in coastal regions which provide valuable ecosystem  
49 services (Barbier et al., 2011; Costanza et al., 1997) and are under high anthropogenic impact  
50 (Halpern et al., 2008). Here, we present the first ocean acidification time-series at weekly  
51 frequency for a coastal site in the Mediterranean Sea.

52 Compared to the global ocean, marginal seas serve a critical role in anthropogenic CO<sub>2</sub>  
53 storage via enhanced CO<sub>2</sub> uptake and export to the ocean interior (Lee et al., 2011). As a  
54 marginal sea, the Mediterranean Sea has a naturally high capacity to absorb but also buffer



55 anthropogenic CO<sub>2</sub> (Álvarez et al., 2014; Palmiéri et al., 2015). This is primarily due to the high  
56 total alkalinity ( $A_T$ ) of Mediterranean waters and overturning circulation (Lee et al., 2011;  
57 Palmiéri et al., 2015; Schneider et al., 2010). In the Mediterranean Sea, the salinity- $A_T$   
58 relationship is driven by the addition of river discharge and Black Sea input, which are generally  
59 both high in  $A_T$  (Copin-Montégut, 1993; Schneider et al., 2007). Combined with evaporation,  
60 this results in higher  $A_T$  and salinity in the Mediterranean Sea compared to the Atlantic  
61 Mediterranean source water (Jiang et al., 2014). On average, Mediterranean Sea  $A_T$  is 10 %  
62 higher than in the global ocean (Palmiéri et al., 2015). The surface ocean acidification rate,  
63 estimated at  $\Delta\text{pH}_T$  of -0.08 since 1800, is comparable to that of the global ocean despite a 10%  
64 greater anthropogenic carbon inventory (Palmiéri et al., 2015). Due to its important role in  
65 carbon sequestration and ecological sensitivity to global ocean change with economic impacts  
66 (Lacoue-Labarthe et al., 2016), the Mediterranean Sea is a key location for time-series  
67 measurements.

68 Over the last few years, numerous studies have estimated ocean acidification rates across  
69 the Mediterranean Sea (Table 1). Together, these studies cover various study periods with a  
70 range of techniques yielding different results. For example, estimates of change in pH of bottom  
71 waters since the preindustrial era range between -0.005 to -0.06 (Palmiéri et al., 2015) and as  
72 much as -0.14 (Touratier and Goyet, 2011). Techniques for estimating ocean acidification in the  
73 Mediterranean Sea thus far include: (1) hind-casting, using high-resolution regional circulation  
74 models (Palmiéri et al., 2015), the TrOCA approach as applied to cruise-based profile data  
75 (Krasakopoulou et al., 2011; Touratier and Goyet, 2011; Touratier et al., 2016) and others  
76 (Howes et al., 2015), (2) partially reconstructed time-series (Marcellin Yao et al., 2016), (3)  
77 comparative study periods (Luchetta et al., 2010; Meier et al., 2014), and (4) sensor-based



78 observations over a short study period (Flecha et al., 2015). Ocean acidification time-series of  
79 consistent sampling over many years are lacking for the Mediterranean Sea (The MerMex  
80 Group, 2011), especially along the coast where river discharge influences the carbonate system  
81 (Ingrosso et al., 2016).

82           Compared to the open ocean, shallow coastal sites exhibit natural variability in carbonate  
83 chemistry over annual timeframes (Hofmann et al., 2011; Kapsenberg and Hofmann, 2016;  
84 Kapsenberg et al., 2015), complicating the detection and relevance of open ocean acidification in  
85 isolation of other processes (Duarte et al., 2013). Variability stems from both physical (e.g.,  
86 upwelling, river discharge; Feely et al., 2008; Vargas et al., 2016) and biological processes (e.g.,  
87 primary production, respiration, net calcification). Within watersheds, coastal carbonate  
88 chemistry is affected by eutrophication (Borges and Gypens, 2010; Cai et al., 2011),  
89 groundwater supply (Cai et al., 2003), and land use and rain influence on river alkalinity  
90 (Raymond and Cole, 2003; Stets et al., 2014). Over longer periods, pH can also be influenced by  
91 atmospheric deposition (Omstedt et al., 2015). Introduction of nutrient-rich upwelled- or fresh-  
92 water masses influences biological processes and carbonate chemistry at higher frequencies.  
93 Through primary production and respiration, coastal ecosystems produce pH fluctuations over  
94 hours (e.g., seagrass, kelp) to months (e.g., phytoplankton blooms; Kapsenberg and Hofmann,  
95 2016). Due to existing pH variability in coastal seas, it is necessary to quantify high-frequency  
96 pH variability in order to interpret the pH changes inferred from lower-frequency sampling, at  
97 time-series stations.

98           In this study, we present the first complete time-series data quantifying the present-day  
99 ocean acidification rate for a coastal site in the Mediterranean Sea, based on weekly  
100 measurements of  $A_T$  and  $C_T$  sampled from 2007 through 2015. For a subset of this time-series,



101 we documented pH variability using a SeaFET™ Ocean pH Sensor in order to assess hourly pH  
102 variability. For comparison and consistency with other ocean acidification time-series around the  
103 world, we report rates of change based on anomalies (Bates et al., 2014).

104

## 105 **2. Materials and methods**

### 106 **2.1. Site description**

107 A carbonate chemistry time-series was initiated in 2007 in the NW Mediterranean Sea at  
108 the entrance of the Bay of Villefranche-sur-Mer, France (Fig. 1): Point B station (43.686° N,  
109 7.316° E, 85 m bottom depth). A second site, Environment Observable Littoral buoy (EOL,  
110 43.682° N, 7.319° E, 80 m bottom depth), was used for pH sensor deployment starting in 2014.  
111 These two sites are 435 m apart. The site Point B is an historical sampling point, since 1957,  
112 regarding several oceanographic parameters. A full site description and research history has been  
113 detailed by De Carlo et al. (2013). Briefly, the Bay is a narrow north-south facing inlet with steep  
114 bathymetry and estimated volume of 310 million m<sup>3</sup>. The surrounding region is predominately  
115 composed of limestone with a series of shallow, submarine groundwater karst springs (Gilli,  
116 1995). The North current, a major and structuring counter-clockwise current in the Ligurian Sea,  
117 can sometimes flow close to Point B. The Bay can also be, on occasion, influenced by local  
118 countercurrents. Both of these hydrodynamics movements have signatures of riverine discharge,  
119 which for the Mediterranean Sea are generally high in  $A_T$  (Copin-Montégut, 1993; Schneider et  
120 al., 2007). For example, the Paillon River, 4 km west of Point B and whose plume on occasion  
121 reaches into the Bay (L. Mousseau, pers. obs.), was sampled on 18 Aug 2014 and had a  $A_T$  of  
122  $1585 \pm 0.1 \mu\text{mol kg}^{-1}$  ( $N=2$ , J.-P. Gattuso, unpubl.). Due to low primary productivity, seasonal



123 warming drives the main annual variability in carbonate chemistry at this location (De Carlo et  
124 al., 2013).

125

## 126 **2.2. Point B data collection, processing, and analysis**

127 To document long-term changes in ocean carbonate chemistry at Point B, seawater was  
128 sampled weekly starting in January 2007. Samples were collected at 1 and 50 m, using a 12-L  
129 Niskin bottle at 9:00 local time. Seawater was transferred from the Niskin bottle to 500 mL  
130 borosilicate glass bottles and fixed within an hour via addition of saturated mercuric chloride for  
131 preservation of carbonate parameters, following recommendations by Dickson et al. (2007).  
132 Duplicate samples were collected for each depth. For each sampling event, CTD casts were  
133 performed either with a Seabird 25 or Seabird 25+ profiler whose sensors are calibrated at least  
134 every two years. Accuracy of conductivity (SBE4 sensor) and temperature (SBE3 sensor)  
135 measurements from CTD casts were  $0.0003 \text{ S m}^{-1}$  and  $0.001^\circ\text{C}$ , respectively.

136 Within 6 months of collection, bottle samples were analyzed for  $C_T$  and  $A_T$  via  
137 potentiometric titration following methods described by Edmond (1970) and DOE (1994), by  
138 *Service National d'Analyse des Paramètres Océaniques du CO<sub>2</sub>*, at the Université Pierre et Marie  
139 Curie in Paris, France. Precision of  $C_T$  and  $A_T$  was less than  $3 \mu\text{mol kg}^{-1}$ , and the average  
140 accuracy was 2.6 and  $3 \mu\text{mol kg}^{-1}$ , as compared with seawater certified reference material  
141 (CRM) provided by A. Dickson (Scripps Institution of Oceanography). Only obvious outliers  
142 were omitted from the analyses: three  $C_T$  values at 1 m ( $> 2300 \mu\text{mol kg}^{-1}$ ), one  $A_T$  value at 1 m  
143 ( $> 2900 \mu\text{mol kg}^{-1}$ ), one  $A_T$  value at 50 m ( $< 2500 \mu\text{mol kg}^{-1}$ ). The  $C_T$  and  $A_T$  measurements on  
144 replicates bottle samples were averaged for analyses.



145           Calculations of the carbonate system parameters were performed using the R package  
146 seacarb version 3.1 with  $C_T$ ,  $A_T$ , temperature and salinity as inputs (Gattuso et al., 2016). Total  
147 concentrations of silicate ( $\text{SiOH}_4$ ) and phosphate ( $\text{PO}_4^{3-}$ ) were used when available from Point B  
148 (L. Mousseau, unpubl.). Detection limits for nutrients were  $0.05 \mu\text{M}$  for  $\text{SiOH}_4$  and  $0.003$  to  
149  $0.006 \mu\text{M}$  for  $\text{PO}_4^{3-}$ ; relative precision of these analyses is 5-10 % (Aminot and K erouel, 2007).  
150 Total boron concentration was calculated from salinity using the global ratio determined by Lee  
151 et al. (2010). The following constants were used:  $K_1$  and  $K_2$  from Lueker et al. (2000),  $K_f$  from  
152 Perez and Fraga (1987), and  $K_s$  from Dickson (1990). Reported measured parameters are  
153 temperature, salinity,  $A_T$ , and  $C_T$ , and derived parameters are  $\text{pH}_T$  (total hydrogen ion scale),  $\text{pH}_T$   
154 normalized to  $25^\circ\text{C}$  ( $\text{pH}_{T25}$ ),  $\text{pCO}_2$ , and aragonite ( $\Omega_a$ ) and calcite ( $\Omega_c$ ) saturation states. Salinity-  
155 normalized changes in  $A_T$  ( $nA_T$ ) and  $C_T$  ( $nC_T$ ) were calculated by dividing by salinity and  
156 multiplying by 38. Except for  $\text{pH}_{T25}$ , all parameters are reported at *in situ* temperatures.

157           The average uncertainties of the derived carbonate parameters were calculated according  
158 to the Gaussian method (Dickson and Riley, 1978) implemented in the “errors” function of the R  
159 package seacarb 3.1 (Gattuso et al., 2016). The uncertainties are  $\pm 2.7 \times 10^{-10} \text{ mol H}^+$  (about  
160  $0.015$  units  $\text{pH}_T$ ),  $\pm 15 \mu\text{atm pCO}_2$ , and  $\pm 0.1$  unit of the aragonite and calcite saturation states.

161           To quantify interannual changes in carbonate parameters, the data were detrended for  
162 seasonality by subtracting monthly means from the time-series following methods in Bates et al.  
163 (2014). The resulting anomalies were analyzed using a linear regression. All analyses were  
164 performed in R (R Core Team, 2016).

165

166   **2.3. Deconvolution of  $\text{pH}_T$  and  $\text{pCO}_2$**



167 To identify proportional contributions of various drivers to ocean acidification trends at  
 168 Point B, deconvolution of time-series  $\text{pH}_T$  and  $\text{pCO}_2$  was performed following methods from  
 169 García-Ibáñez et al. (2016) for observations at 1 m. The equation is described below for  $\text{pH}_T$ ,  
 170 where changes in  $\text{pH}_T$  are driven by changes in temperature ( $T$ ), salinity ( $S$ ),  $A_T$ , and  $C_T$ , over  
 171 time ( $t$ ), according to the following model:

$$172 \quad \frac{d\text{pH}_T}{dt} = \frac{\partial \text{pH}_T}{\partial T} \frac{dT}{dt} + \frac{\partial \text{pH}_T}{\partial S} \frac{dS}{dt} + \frac{\partial \text{pH}_T}{\partial A_T} \frac{dA_T}{dt} + \frac{\partial \text{pH}_T}{\partial C_T} \frac{dC_T}{dt} \quad (1)$$

173 Here,  $\frac{\partial \text{pH}_T}{\partial \text{var}} \frac{d\text{var}}{dt}$  represents the slope contribution of changing  $\text{var}$  to the estimated change  
 174 in  $\text{pH}_T$ , where  $\text{var}$  is either  $T$ ,  $S$ ,  $A_T$ , or  $C_T$ . The rate of pH change due to  $\text{var}$  ( $\frac{\partial \text{pH}_T}{\partial \text{var}} \frac{d\text{var}}{dt}$ ) was  
 175 estimated by calculating  $\text{pH}_T$  using the true observations of  $\text{var}$  but monthly mean values of the  
 176 other three variables, and regressing it to time. The calculation was repeated for  $\text{pCO}_2$  ( $\frac{d\text{pCO}_2}{dt}$ ) in  
 177 order to compare the rate of increase with that of atmospheric  $\text{CO}_2$ .

178 As a sub-component of  $\frac{\partial \text{pCO}_2}{\partial C_T} \frac{dC_T}{dt}$ , the rate of anthropogenic  $\text{CO}_2$  increase was estimated  
 179 from atmospheric  $\text{CO}_2$  concentrations nearest to Point B (Plateau Rosa, Italy, courtesy of the  
 180 World Data Center for Greenhouse Gases, <http://ds.data.jma.go.jp/gmd/wdcgg/>). For these data,  
 181 missing daily values were linearly interpolated. A linear regression was performed where the  
 182 slope represents the rate of  $\text{CO}_2$  increase in the atmosphere. Finally, to help identify different  
 183 processes that might have contributed to the observed trends, linear regressions were performed  
 184 on change in  $A_T$  and  $C_T$  by month and on the salinity- $A_T$  relationship by year.

185

#### 186 **2.4. SeaFET data collection, processing, and analysis**

187 To capture pH variability at higher-than-weekly sampling frequencies, a SeaFET™  
 188 Ocean pH sensor (Satlantic) was deployed on the EOL buoy (435 m from the Point B sampling



189 site) starting in June 2014, at 2 m depth. Autonomous sampling was hourly and deployment  
190 periods ranged between 1 and 3 months. Field calibration samples for pH were collected weekly,  
191 using a Niskin bottle next to SeaFET within 15 min of measurement. This sampling scheme was  
192 sufficient for this site as there is no large high-frequency pH variability. Unlike Point B  
193 sampling, SeaFET calibration samples were processed for pH using the spectrophotometric  
194 method (Dickson et al., 2007) with purified m-cresol purple (purchased from the Byrne lab,  
195 University of South Florida). *In situ* temperature, salinity, and  $A_T$  measured at Point B, within 30  
196 min of the SeaFET sampling, were used to calculate *in situ*  $pH_T$  of the calibration samples.  
197 SeaFET voltage was converted to  $pH_T$  using the respective calibration samples for each  
198 deployment period, following the methods and code described in Bresnahan et al. (2014) but  
199 adapted for use in R.

200 The estimated standard uncertainty in SeaFET  $pH_T$  is  $\pm 0.01$  and was calculated as the  
201 square root of the sum of each error squared. The sources of errors are: measurement error of  
202 spectrophotometric pH ( $\pm 0.004$ ,  $N=68$  mean SD of 5 replicate measurements per calibration  
203 sample for samples collected between 16 July 2014 and 3 May 2016), spatio-temporal mismatch  
204 sampling at EOL ( $\pm 0.007$ , mean offset of  $pH_T$  of the calibration samples from calibrated time-  
205 series), and variability in purified m-cresol dye batch accuracy as compared to Tris buffer CRM  
206 pH ( $\pm 0.006$ , mean offset of  $pH_T$  of the spectrophotometric measurement of Tris buffer from the  
207 CRM value).

208

### 209 3. Results

#### 210 3.1. Time-series trends



211 At Point B from January 2007 to December 2015, >400 samples were collected for  
212 carbonate chemistry at both 1 and 50 m. Anomaly trends detected at 1 m (Fig. 2, Table 2) were  
213 also significant at 50 m (Table S1, Fig. S1), with the exception that salinity increased at 50 m  
214 ( $0.0063 \pm 0.0020$  units  $\text{yr}^{-1}$ ,  $P = 0.002$ ). Changes in carbonate chemistry were faster at 1 m  
215 compared to 50 m, with the exception of salinity and temperature. The warming rate at 50 m was  
216 22 % greater compared to 1 m, mostly due to increasing summer temperatures since 2007.  
217 Analyses for 50 m are available (Table S1, Fig. S1) but here, we focus on results from 1 m unless  
218 explicitly specified otherwise (Fig. 2, Table 2). For time-series anomalies at 1 m, carbonate  
219 chemistry anomalies were significant for  $\text{pH}_T$  ( $-0.0028 \pm 0.0003$  units  $\text{yr}^{-1}$ ,  $N=412$ ),  $A_T$  ( $+2.08 \pm$   
220  $0.19$   $\mu\text{mol kg}^{-1} \text{yr}^{-1}$ ,  $N=417$ ),  $C_T$  ( $+2.97 \pm 0.20$   $\mu\text{mol kg}^{-1} \text{yr}^{-1}$ ,  $N=416$ ),  $\text{pCO}_2$  ( $+3.53 \pm 0.39$   $\mu\text{atm}$   
221  $\text{yr}^{-1}$ ,  $N=412$ ), and  $\Omega_a$  ( $-0.0064 \pm 0.0015$  units  $\text{yr}^{-1}$ ,  $N=412$ ). At the same time, temperature  
222 anomaly increased ( $+0.072 \pm 0.022$   $^\circ\text{C yr}^{-1}$ ,  $N=413$ ), but this significance was lost with the  
223 exclusion of the year 2015 (analysis not shown; changes in other carbonate chemistry parameters  
224 remained significant). No significant change in the salinity anomaly was detected ( $P=0.702$ ,  
225  $N=417$ ).

226 Strong seasonal cycles in carbonate parameters were present at Point B at 1 m (Fig. 3).  
227 Calculated monthly means (2007-2015) are described briefly and listed in Table S2. Mean  
228 temperature range was  $11.2$   $^\circ\text{C}$  with a maximum at  $24.77 \pm 1.35$   $^\circ\text{C}$  in August and minimum of  
229  $13.58 \pm 0.41$   $^\circ\text{C}$  in February. The range in  $A_T$  was  $+19$   $\mu\text{mol kg}^{-1}$  from June to September. The  
230  $C_T$  range was  $33$   $\mu\text{mol kg}^{-1}$  with a peak in late winter and minimum values in August and  
231 October. The opposing seasonal cycles of temperature and  $C_T$ , due to summer warming  
232 coinciding with the period of peak primary productivity (De Carlo et al. 2013), resulted in an  
233 annual  $\text{pH}_T$  range of 0.12 with peak pH in late winter ( $8.14 \pm 0.01$ , February and March) and



234 minimum pH in summer ( $8.02 \pm 0.03$ , July and August). The corresponding pCO<sub>2</sub> range was  
235 +128 μatm from February to August. The monthly means were subtracted from the time-series to  
236 calculate anomalies.

237

### 238 3.2. Deconvolution of pH<sub>T</sub> and pCO<sub>2</sub>

239 Deconvolutions of pH and pCO<sub>2</sub> are presented in Table 3. For both  $\frac{dpH_T}{dt}$  and  $\frac{dpCO_2}{dt}$ ,  
240 temperature and salinity had contributing (approx. 35% and 5% respectively) but non-significant  
241 effects. The 2007-2015 observation period is likely not long enough to detect significance of the  
242 relatively large temperature contribution to  $\frac{dpH_T}{dt}$ . The predominant driver of  $\frac{dpH_T}{dt}$  and  $\frac{dpCO_2}{dt}$  was  
243 the increase in  $C_T$  ( $P \ll 0.001$ ), 56 and 60 % of which was compensated for by a significant  
244 increase in  $A_T$  ( $P = 0.002$ ), respectively.

245 Atmospheric CO<sub>2</sub> at Plateau Rosa increased by  $2.02 \pm 0.03$  ppm yr<sup>-1</sup> ( $F_{1,3285} = 5852.43$ ,  $P$   
246  $\ll 0.001$ ,  $R^2$  0.64), with an anomaly rate of  $2.08 \pm 0.01$  ppm yr<sup>-1</sup> ( $F_{1,3285} = 46649.79$ ,  $P \ll 0.001$ ,  
247  $R^2$  0.93) during the study period 2007-2015, and represents the anthropogenic CO<sub>2</sub> forcing of  
248 ocean acidification. Considering the error associated with deconvolution of pCO<sub>2</sub> and assuming  
249 air-sea CO<sub>2</sub> equilibrium, atmospheric CO<sub>2</sub> increase represents 31 to 44 % of the total  $C_T$   
250 contribution ( $\frac{\partial pCO_2}{\partial C_T} \frac{dC_T}{dt}$ ) to  $\frac{dpCO_2}{dt}$ . This leaves 56 to 69 % of the total  $C_T$  contribution to pCO<sub>2</sub>  
251 unaccounted for. As  $A_T$  is not influenced by addition of anthropogenic CO<sub>2</sub> to seawater, the next  
252 question was, thus, whether or not the changes in  $A_T$  and  $C_T$  were process-linked. Regressions of  
253 annual monthly observations of  $A_T$  and  $C_T$  revealed similar seasonal cycles for both parameters  
254 (Fig. 4). The fastest increases occurred simultaneously for both parameters, which peaked in  
255 June. The smallest changes occurred in January. Significant increases in  $A_T$  occurred from May



256 to July. Significant increases in  $C_T$  occurred from February-August and in November. Results of  
257 regression analyses on monthly changes are listed in Table S3.

258

### 259 **3.3. Salinity and $A_T$ relationships**

260 Given the coastal locale and the increase in  $A_T$ , it is interesting to look at the interannual  
261 variability of the relationship between salinity and  $A_T$  (Fig. 5). With the exception of 2007,  
262 salinity was a poor predictor of  $A_T$ . The  $R^2$  value for each annual salinity- $A_T$  linear regression  
263 ranged from 0.00 (in 2013) to 0.87 (in 2007) with y-intercepts ( $A_{T0}$ , the freshwater end-member  
264 alkalinity) ranging between  $-176 \mu\text{mol kg}^{-1}$  (in 2007) and  $2586 \mu\text{mol kg}^{-1}$  (in 2013). The  
265 interannual variability of the salinity- $A_T$  relationship was driven by the variability in  $A_T$  observed  
266 at salinity  $< 38.0$  that was present from November through July.

267 The salinity cycle (monthly means) at Point B was small and ranged from  $37.64 \pm 0.26$  to  
268  $38.21 \pm 0.11$  from May to September, following freshwater input in winter and spring and  
269 evaporation throughout summer and fall (Fig. 3). Highest ( $> 38.0$ ) and most stable salinity  
270 observations were made in August through October, which coincided with the period of  
271 maximum  $A_T$  ( $2562$  and  $2561 \pm 9 \mu\text{mol kg}^{-1}$  in September and October, respectively). Minimum  
272  $A_T$  ( $2543 \pm 14 \mu\text{mol kg}^{-1}$ ) was observed in June. The reported salinity- $A_T$  relationship is thus  
273 generated from monthly means ( $R^2 = 0.74$ ) where  $A_T$  units are  $\mu\text{mol kg}^{-1}$  and error terms are SE:

$$274 \quad A_T = 1554.9(\pm 185.9) + 26.3(\pm 4.9) \times S \quad (2)$$

275

### 276 **3.4. High-frequency pH data**

277 To verify the weekly sampling scheme at Point B, a total of 11 SeaFET deployments  
278 were conducted from June 2014 to April 2016, averaging  $58 \pm 25$  days and  $5 \pm 2$  calibration



279 samples per deployment (Fig. 6). Only 5 % of the data was removed during quality control, due  
280 to biofouling in one deployment and a drained battery in another, yielding 610 days of good data.  
281 The mean offset between calibration samples and the calibrated SeaFET pH time-series was  $\pm$   
282 0.007 units  $\text{pH}_T$ , indicating a high-quality pH dataset (Fig. 6c). Sensor data corroborated the  
283 seasonal pH and temperature cycle observed at Point B. Event-scale effects (e.g.,  $\text{pH}_T$  change  $\geq$   
284 0.1 for days to weeks, *sensu* Kapsenberg and Hofmann 2016) were absent at this site suggesting  
285 that weekly sampling was sufficient to describe seasonal and interannual changes in carbonate  
286 chemistry at Point B. Magnitude of diel  $\text{pH}_T$  variability was small (the 2.5<sup>th</sup> to 97.5<sup>th</sup> percentiles  
287 ranged between 0.01 and 0.05 units  $\text{pH}_T$ ) and unrelated to seasonal warming or the concentration  
288 of Chlorophyll-a (Fig. S2).

289

## 290 4. Discussion

### 291 4.1. Observed changes in carbonate chemistry

292 Anthropogenic forcing of  $\text{CO}_2$  in seawater necessitates long-term monitoring, in order to  
293 understand and study future ecological change in the coastal environment. In the coastal NW  
294 Mediterranean Sea at EOL, near Point B, high-frequency pH data validated that weekly, morning  
295 sampling at Point B was sufficient to capture water mass changes that were independent from  
296 benthic, diel pH variability in seagrass beds inside the bay (Cox et al., 2016). Based on weekly  
297 samples collected from 2007 through 2015, we detected anomaly changes in  $\text{pH}_T$  of  $-0.0028 \pm$   
298  $0.0003 \text{ units yr}^{-1}$  and an increase in  $A_T$  of  $2.08 \pm 0.19 \mu\text{mol kg}^{-1} \text{ yr}^{-1}$ . The corresponding  $\text{pCO}_2$   
299 increase of  $3.53 \pm 0.39 \mu\text{atm yr}^{-1}$  is 70 % greater than the atmospheric  $\text{CO}_2$  anomaly of  $+2.08 \pm$   
300  $0.01 \text{ ppm yr}^{-1}$  at Plateau Rosa, Italy. While Point B is a weak sink for  $\text{CO}_2$  (De Carlo et al.,  
301 2013), the increase in anthropogenic  $\text{CO}_2$  in the atmosphere alone does not account for all of the



302 observed changes in carbonate chemistry at this location. The increase in  $C_T$  was the dominant  
303 driver of  $\text{pH}_T$  change over the study period. An increase in  $A_T$  partially buffered this  $C_T$  increase  
304 such that the observed acidification rate is only slightly larger than those reported at other ocean  
305 time-series sites ( $-0.0026$  to  $-0.0013$  units  $\text{yr}^{-1}$ , Bates et al., 2014). Warming contributed to  
306 approximately 35 % of the pH decline, which agrees well with the 30 % approximation at  
307 DYFAMED, an open-sea site about 50 km offshore from Point B (Marcellin Yao et al., 2016). A  
308 longer time-series of temperature paired with pH observations will be necessary to definitively  
309 characterize this relationship. While anomalously warm summer temperatures in 2015 drove the  
310 warming trends in this study, this region has warmed steadily since 1980 (Parravicini et al.,  
311 2015) and this is observable at 50 m as well (Fig. S1). Finally, the co-evolution of  $A_T$  and  $C_T$   
312 changes suggests that changes in  $C_T$  are also due to increasing  $A_T$ , which includes bicarbonate  
313 ( $\text{HCO}_3^-$ ) and carbonate ( $\text{CO}_3^{2-}$ ) ions (Fig. 4). We assess the spatial extent of these trends and  
314 discuss potential drivers.

315 Fastest rate increases in  $A_T$  and  $C_T$  occurred from May through July; the period of  
316 seasonal transition (Fig. 3). At this time, various biophysical processes force the seasonality of  
317 the carbonate system. In the NW Mediterranean, the main processes governing seasonal  
318 variability in  $A_T$  are evaporation increasing  $A_T$  in summer (i.e., June through September at Point  
319 B) and, to a lesser extent, phytoplankton uptake of nitrate ( $\text{NO}_3^-$ ) and phosphate ( $\text{PO}_4^{3-}$ )  
320 increasing  $A_T$  from January through March (Cossarini et al., 2015). During the transition of these  
321 processes, salinity decreases to a minimum in May, reflecting freshwater input that dilutes  $A_T$  to  
322 minimum values at the start of summer. For  $C_T$ , peak values occur in winter when the water  
323 column is fully mixed (L. Mousseau, unpubl.). Mixing occurs down to more than 2000 m depth a  
324 few 10s of km from the study site and  $C_T$  is up to  $100 \mu\text{mol kg}^{-1}$  higher in deep waters (Copin-



325 Montégut and Bégovic, 2002). Following winter,  $C_T$  declines due to a combination of  
326 phytoplankton bloom carbon uptake and freshwater dilution, until the onset of summer  
327 stratification. Summer warming leads to  $pCO_2$  off-gassing to the atmosphere (De Carlo et al.,  
328 2013), thereby further decreasing  $C_T$ . The increases in  $A_T$  and  $C_T$  from 2007 through 2015 were  
329 more pronounced at 1 m compared to 50 m, suggesting that the driving processes dominate at the  
330 surface.

331 To estimate if the observed trends from Point B were also occurring offshore, we turn to  
332 time-series station DYFAMED, approx. 50 km from Point B (Fig. 1). The acidification rate at  
333 DYFAMED was estimated at  $-0.003 \pm 0.001$  units  $pH\ yr^{-1}$  from 1995 to 2011 (Marcellin Yao et  
334 al., 2016), however, the uncertainty is large and makes the comparison with Point B unreliable.  
335  $A_T$  at the DYFAMED did not change significantly during the period 2007-2014 ( $F_{1,51} 3.204$ ,  $P =$   
336  $0.0794$ ,  $R^2 0.08$ , data from L. Coppola). This suggests that the processes driving changes in  $A_T$   
337 and  $C_T$  at Point B, in addition to being shallow, dissipate offshore.

338 Another coastal area of the Mediterranean Sea, in the North Adriatic Sea, exhibited  
339 similar changes in carbonate chemistry as those observed at Point B. By comparing cruise data  
340 between the winters of 1983 and 2008, Luchetta et al. (2010) determined an acidification rate of  
341  $pH_T -0.0025$  units  $yr^{-1}$  and an increase in  $A_T$  of  $2.98\ \mu mol\ kg^{-1}\ yr^{-1}$  at depths  $< 75$  m. As coastal  
342 sites, Point B and the Gulf of Trieste in the N Adriatic Sea show a strong positive  $A_{T0}$  (i.e.,  
343 freshwater end-member alkalinity) in surface waters (Cantoni et al., 2012; Ingrosso et al., 2016).  
344 In contrast to Point B, the N Adriatic Sea exhibits a negative salinity- $A_T$  relationship and faster  
345  $A_T$  increase (Luchetta et al., 2010), suggesting that rivers may play a stronger role in  $A_T$  trends  
346 there compared to Point B. Rivers are significant sources of  $C_T$  to the Gulf of Trieste, making up  
347 3-16 % of  $C_T$  in 2007 (Tamše et al., 2015). The authors note that 2007 was a year of record low



348 river discharge. Notably, this is the only year at Point B for which  $A_{T0}$  was negative and salinity-  
349  $A_T$  relationship was highly correlated, also indicating that 2007 was a year of low freshwater  
350 input.

351 The correlates between Point B and N Adriatic Sea suggest a common driver of changes  
352 in ocean carbonate chemistry at these two sites (possibly linked via shared watersheds of the  
353 Alps), and these independent studies may be symptomatic of changes occurring across wider  
354 coastal areas of the Mediterranean Sea. Monitoring efforts of carbonate chemistry in the eastern  
355 Mediterranean Sea would offer an important contrast, as pH of eastern waters is expected to be  
356 more sensitive to atmospheric  $\text{CO}_2$  addition due to their ability to absorb more anthropogenic  
357  $\text{CO}_2$  than either the western Mediterranean or Atlantic waters (Álvarez et al., 2014).

358

#### 359 **4.2. Potential drivers of changes in carbonate chemistry**

360 Coastal ocean acidification rates vary greatly across different regions. In the NW Pacific  
361 coast, rapid acidification of surface waters ( $\Delta\text{pH}_T -0.058$  units  $\text{yr}^{-1}$ ) at Tatoosh Island has been  
362 documented in the absence of concomitant changes in known drivers of local pH variability (e.g.,  
363 upwelling, eutrophication, and more; Wootton and Pfister, 2012; Wootton et al., 2008). Further  
364 inshore, in the Hood Canal sub-basin of the Puget Sound, only 24-49 % of the estimated pH  
365 decline from pre-industrial values could be attributed to anthropogenic  $\text{CO}_2$  (Feely et al., 2010).  
366 The excess decrease in pH was attributed to increased remineralization (Feely et al., 2010).  
367 Acidification rates documented along the North Sea Dutch coastline and inlets were highly  
368 variable in space, with some exceeding the expected anthropogenic  $\text{CO}_2$  rate by an order of  
369 magnitude while others exhibited an increase in pH (Provoost et al., 2010). These sites  
370 experience much greater sub-annual variability than Point B. As a coastal ocean acidification



371 monitoring site, the relative simplicity of the Point B pH variability regime may therefore  
372 provide an opportunity to further investigate the underlying drivers of rapid coastal ocean  
373 acidification in the absence of additional noise from otherwise overshadowing processes.

374 While ocean acidification is often described in  $\text{pH}_T$ , at Point B, pH is largely a product of  
375 underlying changes in  $A_T$  and  $C_T$ . Sediment dissolution is unlikely to contribute to the observed  
376 increase in  $A_T$  as both aragonite and calcite were supersaturated throughout the study period;  
377 conditions that are not conducive to large rates of dissolution. An overall reduction in calcium  
378 carbonate ( $\text{CaCO}_3$ ) precipitation rates is unlikely, as the dominant ecosystem in the Bay of  
379 Villefranche-sur-Mer is seagrass meadows, which harbor relatively few calcifying organisms and  
380 there has been no obvious changes in the abundance of calcifiers (J.-P. Gattuso, pers. obs.). All  
381 the same, the sheer volume of the Bay would likely dilute any signature of changes in  
382 calcification or dissolution of sediment or organisms. For the Mediterranean Sea, in general, the  
383 influence of biogenic  $\text{CaCO}_3$  on  $A_T$  is small compared to the influence of river and Black Sea  $A_T$   
384 (Copin-Montégut, 1993). Increased input from the eastern Mediterranean Sea waters could  
385 increase  $A_T$ , but this is questionable, because while eastern waters are higher in  $A_T$ , salinity and  
386 pH are also greater and  $C_T$  is a little lower, compared to the western waters (Álvarez et al., 2014;  
387 Touratier and Goyet, 2011).

388 For  $C_T$ , there are a few additional drivers to discuss. First, anthropogenic  $\text{CO}_2$  partly  
389 accounted for the observed increase in  $C_T$ , independent of  $A_T$ . In summer,  $\text{pCO}_2$  peaks and Point  
390 B becomes a weak source of  $\text{CO}_2$  to the atmosphere (De Carlo et al., 2013). As atmospheric  $\text{CO}_2$   
391 is increasing it may contribute to summertime  $C_T$  retention, but this effect is likely too small for  
392 the observed increases in  $C_T$ . Second, increased remineralization rates could contribute to  $C_T$ ,  
393 particularly in summer when the water is warmer, hence promoting respiration, and highly



394 stratified and isolated from  $C_T$ -rich bottom waters. However, this would require either (1) a  
395 change in substrate (local or regional) for remineralization but no clear trend in particulate  
396 organic carbon was observable in the study period (L. Mousseau, unpubl.), or (2) a change in net  
397 community metabolism, but warming trends up through 2014 were not significant. Lastly,  
398 Chlorophyll-a biomass, a proxy of primary production, has decreased since 1995 and blooms  
399 have shifted towards earlier dates in the year, at Point B (Irisson et al., 2012). Both of these  
400 processes could influence the increasing rate of  $C_T$  in summer but would not account for the  
401 increase in  $A_T$ .

402 The lack of salinity change excludes additional processes as drivers of carbonate  
403 chemistry change at Point B. For example, increased summertime evaporation (concentration  
404 effect) and reduced riverine discharge (decreased dilution effect) would both be expected to  
405 cause an increase in salinity, which was not observed and so these are not suspected drivers.  
406 However, changes in the content of freshwater sources is conceivable.

407 The observed changes in  $A_T$  and  $C_T$  could be achieved via augmented limestone  
408 weathering increasing the  $A_T$  input from land to the sea via rivers and submarine groundwater  
409 springs. Increased  $A_T$  in freshwater was documented in North American rivers (Raymond and  
410 Cole, 2003; Stets et al., 2014) and groundwater (Macpherson et al., 2008). For the Mediterranean  
411 Sea, rivers are a significant source of both  $A_T$  and  $C_T$  (Copin-Montégut, 1993). Riverine  
412 contributions of  $A_T$  originate from erosion and are correlated with bedrock composition (e.g.,  
413 McGrath et al., 2016). The annual variability in salinity- $A_T$  relationships at Point B does suggest  
414 influence of river discharge, as has been observed elsewhere in the Mediterranean Sea (Cantoni  
415 et al., 2012; Turk et al., 2010). Signatures of limestone erosion can be observed in the  $A_T$  of local  
416 rivers near Point B (Var, Paillon, and Roya) and range between 1000 to 2000  $\mu\text{mol kg}^{-1}$  (data



417 from *Agence de l'Eau Rhône-Méditerranée-Corse*, <http://sierm.eaurmc.fr>). Even a rainwater  
418 outfall at the entrance of Port de la Darse harbor, inside the Bay of Villefranche-sur-Mer, had an  
419  $A_T$  of  $607 \pm 5 \mu\text{mol kg}^{-1}$  ( $N=2$ ) following a precipitation event. However, local precipitation was  
420 not correlated with salinity or  $A_T$ , suggesting that rain runoff is not a driving factor of Point B  
421 carbonate chemistry (Fig. S3). Lastly, submarine groundwater springs are a significant source of  
422 nutrients,  $A_T$ , and  $C_T$  to the ocean (Cai et al., 2003; Slomp and Van Cappellen, 2004). Submarine  
423 springs have been identified along the Point B coastline (Gilli, 1995), but their carbonate  
424 chemistry contributions are currently unknown.

425 Rivers as a potential driver of  $A_T$  and  $C_T$  trends at Point B could be achieved if the  $A_T$   
426 content discharged by rivers was changing, as was proposed for the Adriatic Sea (Luchetta et al.,  
427 2010). For example, terrestrial organic matter cycling influences riverine  $C_T$  (Vargas et al.,  
428 2016), so changes in soil respiration could be expected to change  $A_T$  of rivers. Increasing river  $A_T$   
429 has been documented in North America and occurs via a number of processes including: (1) the  
430 interplay of rainfall and land-use (Raymond and Cole, 2003), (2) anthropogenic limestone  
431 addition (a.k.a., liming) used to enhance agriculture soil pH (Oh and Raymond, 2006; Stets et al.,  
432 2014) and freshwater pH (Clair and Hindar, 2005), and (3) potentially indirect effects of  
433 anthropogenic  $\text{CO}_2$  on groundwater  $\text{CO}_2$ -acidification and weathering (Macpherson et al., 2008).  
434 Such, and other, processes are hypothesized to have driven  $A_T$  changes in the Baltic Sea (Müller  
435 et al., 2016). There,  $A_T$  increased at a rate of  $+3.4 \mu\text{mol kg}^{-1} \text{ yr}^{-1}$  during the period 1995 to 2014  
436 (mean salinity = 7). In contrast to Point B, where salinity is about 38, the increase in Baltic Sea  
437  $A_T$  was not noticeable at salinity  $> 30$  (Müller et al., 2016). This contrast clouds the perspective  
438 that changes in  $A_T$  of freshwater sources can influence  $A_T$  at Point B, and a more in depth study  
439 will be necessary to address this.



440           Given the discussion above, the simplest plausible mechanisms causing changes in  
441 carbonate chemistry at Point B would be through (1) increasing anthropogenic atmospheric CO<sub>2</sub>,  
442 and (2) increasing  $A_T$  of freshwater sources (i.e., rivers, groundwater). Freshwater has a shallow  
443 and coastal influence and is also dominant in the N Adriatic Sea, which exhibits similar trends as  
444 those observed at Point B. If so, there is a lag effect, as freshwater influence peaks in May but  $A_T$   
445 and  $C_T$  increased fastest from May through July. Consequently, this hypothesis needs further  
446 investigation. The influence of a coastal boundary processes influencing seawater  $A_T$  and  $C_T$   
447 presents a potentially major difference between coastal and offshore ocean acidification rates.  
448 Until the source of  $A_T$  increase is properly identified, use of this observation (e.g., in modeling)  
449 should be implemented with great caution.

450

## 451 **5. Conclusion**

452           Predictions of coastal ocean acidification remain challenging due the complexity of  
453 biogeochemical processes occurring at the ocean-land boundary and the lack of long-term  
454 monitoring. At the Point B coastal monitoring station in the NW Mediterranean Sea, the ocean  
455 acidification trend is greater than expected from assuming atmospheric equilibrium. We  
456 postulate that the enhanced acidification trend could stem from changes in freshwater inputs  
457 from land which are also the source of interannual variability in  $A_T$  at this site. This study  
458 highlights the importance of considering other anthropogenic influences in the greater land-sea  
459 region that may (1) contribute to coastal biogeochemical cycles (*sensu* Duarte et al. 2013) and  
460 (2) inform projections of anthropogenic change in near-shore waters and experimental design in  
461 global ocean change biology.

462



463 **Data availability** – Time-series data from Point B are available at Pangaea<sup>®</sup> (doi:

464 10.1594/PANGAEA.727120)

465

466 **Author contribution** – JPG initiated the study, LM supervised data collection, SA performed

467 SeaFET deployments and calibration, JPG and LK designed and JPG conducted statistical

468 analyses, and LK prepared the manuscript with contributions from all authors.

469

470 **Competing interests** - The authors declare that they have no conflict of interest.

471

472 **Acknowledgements** – Thanks are due to the Service d'Observation Rade de Villefranche (SO-

473 Rade) of the Observatoire Océanologique and the Service d'Observation en Milieu Littoral

474 (SOMLIT/CNRS-INSU) for their kind permission to use the Point B data. Bottle samples were

475 analyzed for  $C_T$  and  $A_T$  by the *Service National d'Analyse des Paramètres Océaniques du CO<sub>2</sub>*.

476 Thanks are also due to Jean-Yves Carval, Anne-Marie Corre, Maïa Durozier, Ornella Passafiume

477 and Frank Petit for sampling assistance, to Alice Webb for her help with data analysis and to

478 Bernard Gentili and Jean-Olivier Irisson for producing Figure 1. Atmospheric CO<sub>2</sub> data from

479 Plateau Rosa was collected by Ricerca sul Sistema Energetico (RSE S.p.A.); we are grateful for

480 their contribution. The authors acknowledge L. Coppola for providing DYFAMED data and

481 Météo-France for supplying the meteorological data and the HyMeX database teams

482 (ESPRI/IPSL and SEDOO/Observatoire Midi-Pyrenees) for their help in accessing them. The

483 *Agence de l'Eau Rhône-Méditerranée-Corse* kindly provided data on the chemistry of local

484 rivers. Alexandre Dano, Gilles Dandec and Dominique Chassagne provided the high-resolution

485 bathymetric data for the volume estimate of the Bay. We are grateful for helpful comments from



486 Nicolas Metzl on the manuscript. This work is a contribution to the European Project on Ocean  
487 Acidification (EPOCA; contract # 211384) and the MedSeA project (contract # 265103), which  
488 received funding from the European Community's Seventh Framework Programme, and to the  
489 United States National Science Foundation Ocean Sciences Postdoctoral Research Fellowship  
490 (OCE-1521597) awarded to LK.

491

#### 492 **References**

- 493 Álvarez, M., Sanleón-Bartolomé, H., Tanhua, T., Mintrop, L., Luchetta, A., Cantoni, C.,  
494 Schroeder, K., and Civitarese, G.: The CO<sub>2</sub> system in the Mediterranean Sea: a basin  
495 wide perspective, *Ocean Sci.*, 10, 69-92, 10.5194/os-10-69-2014, 2014.
- 496 Aminot, A., and Kérouel, R.: Dosage automatique des nutriments dans les eaux marines:  
497 méthodes d'analyse en milieu marin, edited by: Ifremer, 188 pp pp., 2007.
- 498 Barbier, E. B., Hacker, S. D., Kennedy, C., Koch, E. W., Stier, A. C., and Silliman, B. R.: The  
499 value of estuarine and coastal ecosystem services, *Ecol. Monogr.*, 81, 169-193,  
500 10.1890/10-1510.1, 2011.
- 501 Bates, N. R., Astor, Y. M., Church, M. J., Currie, K., Dore, J. E., González-Dávila, M.,  
502 Lorenzoni, L., Muller-Karger, F., Olafsson, J., and Santana-Casiano, J. M.: A time-series  
503 view of changing ocean chemistry due to ocean uptake of anthropogenic CO<sub>2</sub> and ocean  
504 acidification, *Oceanography*, 27, 126-141, 2014.
- 505 Borges, A. V., and Gypens, N.: Carbonate chemistry in the coastal zone responds more strongly  
506 to eutrophication than ocean acidification, *Limnol. Oceanogr.*, 55, 346-353,  
507 10.4319/lo.2010.55.1.0346, 2010.



- 508 Bresnahan, P. J., Martz, T. R., Takeshita, Y., Johnson, K. S., and LaShomb, M.: Best practices  
509 for autonomous measurement of seawater pH with the Honeywell Durafet, *Methods*  
510 *Oceangr.*, 9, 44-60, 2014.
- 511 Cai, W.-J., Wang, Y., Krest, J., and Moore, W. S.: The geochemistry of dissolved inorganic  
512 carbon in a surficial groundwater aquifer in North Inlet, South Carolina, and the carbon  
513 fluxes to the coastal ocean, *Geochim. Cosmochim. Acta*, 67, 631-639, 10.1016/S0016-  
514 7037(02)01167-5, 2003.
- 515 Cai, W.-J., Hu, X., Huang, W.-J., Murrell, M. C., Lehrter, J. C., Lohrenz, S. E., Chou, W.-C.,  
516 Zhai, W., Hollibaugh, J. T., Wang, Y., Zhao, P., Guo, X., Gundersen, K., Dai, M., and  
517 Gong, G.-C.: Acidification of subsurface coastal waters enhanced by eutrophication,  
518 *Nature Geosci*, 4, 766-770, 10.1038/ngeo1297, 2011.
- 519 Cantoni, C., Luchetta, A., Celio, M., Cozzi, S., Raicich, F., and Catalano, G.: Carbonate system  
520 variability in the Gulf of Trieste (North Adriatic Sea), *Estuar. Coast. Shelf Sci.*, 115, 51-  
521 62, 10.1016/j.ecss.2012.07.006, 2012.
- 522 Clair, T. A., and Hindar, A.: Liming for the mitigation of acid rain effects in freshwaters: a  
523 review of recent results, *Environ. Rev.*, 13, 91-128, 10.1139/a05-009, 2005.
- 524 Copin-Montégut, C.: Alkalinity and carbon budgets in the Mediterranean Sea, *Global*  
525 *Biogeochem. Cycles*, 7, 915-925, 10.1029/93GB01826, 1993.
- 526 Copin-Montégut, C., and Bégovic, M.: Distributions of carbonate properties and oxygen along  
527 the water column (0–2000 m) in the central part of the NW Mediterranean Sea (Dyfamed  
528 site): influence of winter vertical mixing on air–sea CO<sub>2</sub> and O<sub>2</sub> exchanges, *Deep-Sea*  
529 *Research Part II: Topical Studies in Oceanography*, 49, 2049-2066, 10.1016/S0967-  
530 0645(02)00027-9, 2002.



- 531 Cossarini, G., Lazzari, P., and Solidoro, C.: Spatiotemporal variability of alkalinity in the  
532 Mediterranean Sea, *Biogeosciences*, 12, 1647-1658, 10.5194/bg-12-1647-2015, 2015.
- 533 Costanza, R., d'Arge, R., de Groot, R., Farber, S., Grasso, M., Hannon, B., Limburg, K., Naeem,  
534 S., O'Neill, R. V., Paruelo, J., Raskin, R. G., Sutton, P., and van den Belt, M.: The value  
535 of the world's ecosystem services and natural capital, *Nature*, 387, 253-260, 1997.
- 536 Cox, T. E., Gazeau, F., Alliouane, S., Hendriks, I. E., Mahacek, P., Le Fur, A., and Gattuso, J.-  
537 P.: Effects of in situ CO<sub>2</sub> enrichment on structural characteristics, photosynthesis, and  
538 growth of the Mediterranean seagrass *Posidonia oceanica*, *Biogeosciences*, 13, 2179-  
539 2194, 10.5194/bg-13-2179-2016, 2016.
- 540 De Carlo, E. H., Mousseau, L., Passafiume, O., Drupp, P. S., and Gattuso, J.-P.: Carbonate  
541 chemistry and air-sea CO<sub>2</sub> flux in a NW Mediterranean bay over a four-year period:  
542 2007–2011, *Aquatic Geochemistry*, 19, 399-442, 10.1007/s10498-013-9217-4, 2013.
- 543 Dickson, A.: The carbon dioxide system in seawater: equilibrium chemistry and measurements,  
544 in: *Guide to best practices for ocean acidification research and data reporting*, edited by:  
545 Fabry, V. J., Hansson, L., and Gattuso, J.-P., Luxembourg: Publications Office of the  
546 European Union, 17-40, 2010.
- 547 Dickson, A. G., and Riley, J. P.: The effect of analytical error on the evaluation of the  
548 components of the aquatic carbon-dioxide system, *Mar. Chem.*, 6, 77-85, 10.1016/0304-  
549 4203(78)90008-7, 1978.
- 550 Dickson, A. G.: Standard potential of the reaction:  $\text{AgCl(s)} + 1/2 \text{H}_2\text{(g)} = \text{Ag(s)} + \text{HCl(aq)}$ , and  
551 and the standard acidity constant of the ion  $\text{HSO}_4^-$  in synthetic sea water from 273.15 to  
552 318.15 K, *The Journal of Chemical Thermodynamics*, 22, 113-127, 10.1016/0021-  
553 9614(90)90074-Z, 1990.



- 554 Dickson, A. G., Sabine, C. L., and Christian, J. R.: Guide to best practices for ocean CO<sub>2</sub>  
555 measurements, PICES Special Publication, 3, 191 pp., 2007.
- 556 DOE: Handbook of methods for the analysis of the various parameters of the carbon dioxide  
557 system in sea water, Carbon Dioxide Information Analysis Center, Oak Ridge National  
558 Laboratory, 1994.
- 559 Doney, S. C., Fabry, V. J., Feely, R. A., and Kleypas, J. A.: Ocean acidification: the other CO<sub>2</sub>  
560 problem, *Ann. Rev. Mar. Sci.*, 1, 169-192, 10.1146/annurev.marine.010908.163834,  
561 2009.
- 562 Duarte, C. M., Hendriks, I. E., Moore, T. S., Olsen, Y. S., Steckbauer, A., Ramajo, L.,  
563 Carstensen, J., Trotter, J. A., and McCulloch, M.: Is ocean acidification an open-ocean  
564 syndrome? Understanding anthropogenic impacts on seawater pH, *Estuaries and Coasts*,  
565 36, 221-236, 10.1007/s12237-013-9594-3, 2013.
- 566 Edmond, J. M.: High precision determination of titration alkalinity and total carbon dioxide  
567 content of sea water by potentiometric titration, *Deep-Sea Research*, 17, 737-750,  
568 10.1016/0011-7471(70)90038-0, 1970.
- 569 Feely, R. A., Sabine, C. L., Hernandez-Ayon, J. M., Ianson, D., and Hales, B.: Evidence for  
570 upwelling of corrosive "acidified" water onto the continental shelf, *Science*, 320, 1490-  
571 1492, 10.1126/science.1155676, 2008.
- 572 Feely, R. A., Alin, S. R., Newton, J., Sabine, C. L., Warner, M., Devol, A., Krembs, C., and  
573 Maloy, C.: The combined effects of ocean acidification, mixing, and respiration on pH  
574 and carbonate saturation in an urbanized estuary, *Estuar. Coast. Shelf Sci.*, 88,  
575 10.1016/j.ecss.2010.05.004, 2010.



- 576 Flecha, S., Pérez, F. F., García-Lafuente, J., Sammartino, S., Ríos, A. F., and Huertas, I. E.:  
577 Trends of pH decrease in the Mediterranean Sea through high frequency observational  
578 data: indication of ocean acidification in the basin, *Sci. Rep.*, 5, 16770,  
579 10.1038/srep16770, 2015.
- 580 García-Ibáñez, M. I., Zunino, P., Fröb, F., Carracedo, L. I., Ríos, A. F., Mercier, H., Olsen, A.,  
581 and Pérez, F. F.: Ocean acidification in the subpolar North Atlantic: rates and  
582 mechanisms controlling pH changes, *Biogeosciences*, 13, 3701-3715, 10.5194/bg-13-  
583 3701-2016, 2016.
- 584 Gattuso, J.-P., Epitalon, J.-M., and Lavigne, H.: seacarb: Seawater Carbonate Chemistry. R  
585 package version 3.0. <https://cran.r-project.org/package=seacarb>, 2016.
- 586 Gattuso, J. P., and Hansson, L.: Ocean acidification, Oxford University Press, Oxford, 2011.
- 587 Gilli, E.: Etude des sources karstiques sous-marines et littorales des Alpes Maritimes entre  
588 Menton et Nice, 41p, 1995.
- 589 Group, T. M., Durrieu de Madron, X., Guieu, C., Sempéré, R., Conan, P., Cossa, D., D'Ortenzio,  
590 F., Estournel, C., Gazeau, F., Rabouille, C., Stemmann, L., Bonnet, S., Diaz, F., Koubbi,  
591 P., Radakovitch, O., Babin, M., Baklouti, M., Bancon-Montigny, C., Belviso, S.,  
592 Bensoussan, N., Bonsang, B., Bouloubassi, I., Brunet, C., Cadiou, J. F., Carlotti, F.,  
593 Chami, M., Charmasson, S., Charrière, B., Dachs, J., Doxaran, D., Dutay, J. C., Elbaz-  
594 Poulichet, F., Eléaume, M., Eyrolles, F., Fernandez, C., Fowler, S., Francour, P.,  
595 Gaertner, J. C., Galzin, R., Gasparini, S., Ghiglione, J. F., Gonzalez, J. L., Goyet, C.,  
596 Guidi, L., Guizien, K., Heimbürger, L. E., Jacquet, S. H. M., Jeffrey, W. H., Joux, F., Le  
597 Hir, P., Leblanc, K., Lefèvre, D., Lejeusne, C., Lemé, R., Loÿe-Pilot, M. D., Mallet, M.,  
598 Méjanelle, L., Mélin, F., Mellon, C., Mériçot, B., Merle, P. L., Migon, C., Miller, W. L.,



- 599 Mortier, L., Mostajir, B., Mousseau, L., Moutin, T., Para, J., Pérez, T., Petrenko, A.,  
600 Poggiale, J. C., Prieur, L., Pujo-Pay, M., Pulido, V., Raimbault, P., Rees, A. P., Ridame,  
601 C., Rontani, J. F., Ruiz Pino, D., Sicre, M. A., Taillandier, V., Tamburini, C., Tanaka, T.,  
602 Taupier-Letage, I., Tedetti, M., Testor, P., Thébault, H., Thouvenin, B., Touratier, F.,  
603 Tronczynski, J., Ulses, C., Van Wambeke, F., Vantrepotte, V., Vaz, S., and Verney, R.:  
604 Marine ecosystems' responses to climatic and anthropogenic forcings in the  
605 Mediterranean, *Prog. Oceanogr.*, 91, 97-166, 10.1016/j.pocean.2011.02.003, 2011.
- 606 Halpern, B. S., Walbridge, S., Selkoe, K. A., Kappel, C. V., Micheli, F., D'Agrosa, C., Bruno, J.  
607 F., Casey, K. S., Ebert, C., and Fox, H. E.: A global map of human impact on marine  
608 ecosystems, *Science*, 319, 948-952, 2008.
- 609 Hofmann, G. E., Smith, J. E., Johnson, K. S., Send, U., Levin, L. A., Micheli, F., Paytan, A.,  
610 Price, N. N., Peterson, B., Takeshita, Y., Matson, P. G., Crook, E. D., Kroeker, K. J.,  
611 Gambi, M. C., Rivest, E. B., Frieder, C. A., Yu, P. C., and Martz, T. R.: High-frequency  
612 dynamics of ocean pH: a multi-ecosystem comparison, *PLoS One*, 6, e28983,  
613 10.1371/journal.pone.0028983, 2011.
- 614 Howes, E. L., Stemmann, L., Assailly, C., Irisson, J. O., Dima, M., Bijma, J., and Gattuso, J. P.:  
615 Pteropod time series from the North Western Mediterranean (1967-2003): impacts of pH  
616 and climate variability, *Mar. Ecol. Prog. Ser.*, 531, 193-206, 2015.
- 617 Ingrosso, G., Giani, M., Comici, C., Kralj, M., Piacentino, S., De Vittor, C., and Del Negro, P.:  
618 Drivers of the carbonate system seasonal variations in a Mediterranean gulf, *Estuar.*  
619 *Coast. Shelf Sci.*, 168, 58-70, 10.1016/j.ecss.2015.11.001, 2016.
- 620 Irisson, J.-O., Webb, A., Passafiume, O., and Mousseau, L.: Detecting hydrologic variations in a  
621 long term monitoring time series, *Europole Mer Gordon-like conference "Time-series*



- 622 analysis in marine science and application for industry", Brest, France, 17-21 Sept 2012,  
623 2012.
- 624 Jiang, Z.-P., Tyrrell, T., Hydes, D. J., Dai, M., and Hartman, S. E.: Variability of alkalinity and  
625 the alkalinity-salinity relationship in the tropical and subtropical surface ocean, *Global*  
626 *Biogeochem. Cycles*, 28, 729-742, 10.1002/2013GB004678, 2014.
- 627 Kapsenberg, L., Kelley, A. L., Shaw, E. C., Martz, T. R., and Hofmann, G. E.: Near-shore  
628 Antarctic pH variability has implications for biological adaptation to ocean acidification,  
629 *Sci. Rep.*, 5, 9638, 10.1038/srep09638, 2015.
- 630 Kapsenberg, L., and Hofmann, G. E.: Ocean pH time-series and drivers of variability along the  
631 northern Channel Islands, California, USA, *Limnol. Oceanogr.*, 61, 953-968,  
632 10.1002/lno.10264, 2016.
- 633 Krasakopoulou, E., Souvermezoglou, E., and Goyet, C.: Anthropogenic CO<sub>2</sub> fluxes in the  
634 Otranto Strait (E. Mediterranean) in February 1995, *Deep-Sea Research Part I:*  
635 *Oceanographic Research Papers*, 58, 1103-1114, 10.1016/j.dsr.2011.08.008, 2011.
- 636 Lacoue-Labarthe, T., Nunes, P. A. L. D., Ziveri, P., Cinar, M., Gazeau, F., Hall-Spencer, J. M.,  
637 Hilmi, N., Moschella, P., Safa, A., Sauzade, D., and Turley, C.: Impacts of ocean  
638 acidification in a warming Mediterranean Sea: An overview, *Regional Studies in Marine*  
639 *Science*, 5, 1-11, 10.1016/j.rsma.2015.12.005, 2016.
- 640 Le Quéré, C., Moriarty, R., Andrew, R., Peters, G., Ciais, P., Friedlingstein, P., Jones, S., Sitch,  
641 S., Tans, P., Arneeth, A., Boden, T., Bopp, L., Bozec, Y., Canadell, J., Chini, L.,  
642 Chevallier, F., Cosca, C., Harris, I., Hoppema, M., Houghton, R., House, J., Jain, A.,  
643 Johannessen, T., Kato, E., Keeling, R., Kitidis, V., Klein Goldewijk, K., Koven, C.,  
644 Landa, C., Landschützer, P., Lenton, A., Lima, I., Marland, G., Mathis, J., Metzl, N.,



- 645 Nojiri, Y., Olsen, A., Ono, T., Peng, S., Peters, W., Pfeil, B., Poulter, B., Raupach, M.,  
646 Regnier, P., Rödenbeck, C., Saito, S., Salisbury, J., Schuster, U., Schwinger, J., Séférian,  
647 R., Segschneider, J., Steinhoff, T., Stocker, B., Sutton, A., Takahashi, T., Tilbrook, B.,  
648 Van Der Werf, G., Viovy, N., Wang, Y., Wanninkhof, R., Wiltshire, A., and Zeng, N.:  
649 Global carbon budget 2014, *Earth System Science Data*, 7, 47-85, 10.5194/essd-7-47-  
650 2015, 2015.
- 651 Lee, K., Kim, T.-W., Byrne, R. H., Millero, F. J., Feely, R. A., and Liu, Y.-M.: The universal  
652 ratio of boron to chlorinity for the North Pacific and North Atlantic oceans, *Geochim.*  
653 *Cosmochim. Acta*, 74, 1801-1811, 10.1016/j.gca.2009.12.027, 2010.
- 654 Lee, K., Sabine, C. L., Tanhua, T., Kim, T.-W., Feely, R. A., and Kim, H.-C.: Roles of marginal  
655 seas in absorbing and storing fossil fuel CO<sub>2</sub>, *Energy & Environmental Science*, 4, 1133-  
656 1146, 10.1039/C0EE00663G, 2011.
- 657 Luchetta, A., Cantoni, C., and Catalano, G.: New observations of CO<sub>2</sub>-induced acidification in  
658 the northern Adriatic Sea over the last quarter century, *Chem. Ecol.*, 26, 1-17,  
659 10.1080/02757541003627688, 2010.
- 660 Lueker, T. J., Dickson, A. G., and Keeling, C. D.: Ocean *p*CO<sub>2</sub> calculated from dissolved  
661 inorganic carbon, alkalinity, and equations for *K*<sub>1</sub> and *K*<sub>2</sub>: validation based on laboratory  
662 measurements of CO<sub>2</sub> in gas and seawater at equilibrium, *Mar. Chem.*, 70, 105-119,  
663 10.1016/S0304-4203(00)00022-0, 2000.
- 664 Macpherson, G. L., Roberts, J. A., Blair, J. M., Townsend, M. A., Fowle, D. A., and Beisner, K.  
665 R.: Increasing shallow groundwater CO<sub>2</sub> and limestone weathering, Konza Prairie, USA,  
666 *Geochim. Cosmochim. Acta*, 72, 5581-5599, 10.1016/j.gca.2008.09.004, 2008.



- 667 Marcellin Yao, K., Marcou, O., Goyet, C., Guglielmi, V., Touratier, F., and Savy, J.-P.: Time  
668 variability of the north-western Mediterranean Sea pH over 1995–2011, *Mar. Environ.*  
669 *Res.*, 116, 51-60, 10.1016/j.marenvres.2016.02.016, 2016.
- 670 McGrath, T., McGovern, E., Cave, R. R., and Kivimäe, C.: The inorganic carbon chemistry in  
671 coastal and shelf waters around Ireland, *Estuaries and Coasts*, 39, 27-39, 10.1007/s12237-  
672 015-9950-6, 2016.
- 673 Meier, K. J. S., Beaufort, L., Heussner, S., and Ziveri, P.: The role of ocean acidification in  
674 *Emiliana huxleyi* coccolith thinning in the Mediterranean Sea, *Biogeosciences*, 11, 2857-  
675 2869, 10.5194/bg-11-2857-2014, 2014.
- 676 Müller, J. D., Schneider, B., and Rehder, G.: Long-term alkalinity trends in the Baltic Sea and  
677 their implications for CO<sub>2</sub>-induced acidification, *Limnol. Oceanogr.*, 10.1002/lno.10349,  
678 2016.
- 679 Oh, N.-H., and Raymond, P. A.: Contribution of agricultural liming to riverine bicarbonate  
680 export and CO<sub>2</sub> sequestration in the Ohio River basin, *Global Biogeochem. Cycles*, 20,  
681 n/a-n/a, 10.1029/2005GB002565, 2006.
- 682 Omstedt, A., Edman, M., Claremar, B., and Rutgersson, A.: Modelling the contributions to  
683 marine acidification from deposited SO<sub>x</sub>, NO<sub>x</sub>, and NH<sub>x</sub> in the Baltic Sea: Past and  
684 present situations, *Cont. Shelf Res.*, 111, Part B, 234-249, 10.1016/j.csr.2015.08.024,  
685 2015.
- 686 Palmiéri, J., Orr, J., Dutay, J., Béranger, K., Schneider, A., Beuvier, J., and Somot, S.: Simulated  
687 anthropogenic CO<sub>2</sub> storage and acidification of the Mediterranean Sea, *Biogeosciences*,  
688 12, 781-802, 2015.



- 689 Parravicini, V., Mangialajo, L., Mousseau, L., Peirano, A., Morri, C., Montefalcone, M.,  
690 Francour, P., Kulbicki, M., and Bianchi, C. N.: Climate change and warm-water species  
691 at the north-western boundary of the Mediterranean Sea, *Mar. Ecol.*, 36, 897-909,  
692 10.1111/maec.12277, 2015.
- 693 Perez, F. F., and Fraga, F.: The pH measurements in seawater on the NBS scale, *Mar. Chem.*, 21,  
694 315-327, 10.1016/0304-4203(87)90054-5, 1987.
- 695 Pörtner, H.-O., Karl, D., Boyd, P. W., Cheung, W., Lluch-Cota, S. E., Nojiri, Y., Schmidt, D. N.,  
696 and Zavialov, P.: Ocean systems, in: *Climate Change 2014: Impacts, Adaptation, and*  
697 *Vulnerability. Part A: Global and Sectoral Aspects. Contribution of Working Group II to*  
698 *the Fifth Assessment Report of the Intergovernmental Panel on Climate Change*, edited  
699 by: Field, C. B., Barros, V. R., Dokken, D. J., Mach, K. J., Mastrandrea, M. D., Bilir, T.  
700 E., Chatterjee, M., Ebi, K. L., Estrada, Y. O., Genova, R. C., Girma, B., Kissel, E. S.,  
701 Levy, A. N., MacCracken, S., Mastrandrea, P. R., and L.L.White, Cambridge University  
702 Press, Cambridge, United Kingdom and New York, NY, USA, 411-484, 2014.
- 703 Provoost, P., van Heuven, S., Soetaert, K., Laane, R. W. P. M., and Middelburg, J. J.: Seasonal  
704 and long-term changes in pH in the Dutch coastal zone, *Biogeosciences*, 7, 3869-3878,  
705 10.5194/bg-7-3869-2010, 2010.
- 706 Raymond, P. A., and Cole, J. J.: Increase in the export of alkalinity from North America's largest  
707 river, *Science*, 301, 88-91, 2003.
- 708 Rhein, M., Rintoul, S. R., Aoki, S., Campos, E., Chambers, D., Feely, R. A., Gulev, S., Johnson,  
709 G. C., Josey, S. A., A. Kostianoy, Mauritzen, C., Roemmich, D., Talley, L. D., and  
710 Wang, F.: Observations: Ocean, in: *Climate Change 2013: The Physical Science Basis.*  
711 *Contribution of Working Group I to the Fifth Assessment Report of the*



- 712 Intergovernmental Panel on Climate Change, edited by: Stocker, T. F., Qin, D., Plattner,  
713 G.-K., Tignor, M., Allen, S. K., Boschung, J., Nauels, A., Xia, Y., Bex, V., and Midgley,  
714 P. M., Cambridge University Press, Cambridge, United Kingdom and New York, NY,  
715 USA., 2013.
- 716 Schneider, A., Wallace, D. W. R., and Körtzinger, A.: Alkalinity of the Mediterranean Sea,  
717 Geophys. Res. Lett., 34, n/a-n/a, 10.1029/2006GL028842, 2007.
- 718 Schneider, A., Tanhua, T., Körtzinger, A., and Wallace, D. W. R.: High anthropogenic carbon  
719 content in the eastern Mediterranean, J. Geophys. Res., 115, n/a-n/a,  
720 10.1029/2010JC006171, 2010.
- 721 Slomp, C. P., and Van Cappellen, P.: Nutrient inputs to the coastal ocean through submarine  
722 groundwater discharge: controls and potential impact, Journal of Hydrology, 295, 64-86,  
723 10.1016/j.jhydrol.2004.02.018, 2004.
- 724 Stets, E. G., Kelly, V. J., and Crawford, C. G.: Long-term trends in alkalinity in large rivers of  
725 the conterminous US in relation to acidification, agriculture, and hydrologic  
726 modification, Sci. Total Environ., 488–489, 280-289, 10.1016/j.scitotenv.2014.04.054,  
727 2014.
- 728 Tamše, S., Ogrinc, N., Walter, L. M., Turk, D., and Faganeli, J.: River sources of dissolved  
729 inorganic carbon in the Gulf of Trieste (N Adriatic): stable carbon isotope evidence,  
730 Estuaries and Coasts, 38, 151-164, 10.1007/s12237-014-9812-7, 2015.
- 731 Tanhua, T., Bates, N. R., and Körtzinger, A.: The marine carbon cycle and ocean anthropogenic  
732 CO<sub>2</sub> inventories, in: Ocean Circulation and Climate: A 21st Century Perspective. 2nd Ed,  
733 edited by: Siedler, G., Griffies, S., Gould, J., and Church, J., 103, Academic Press, 787-  
734 816, 2013.



- 735 Team, R. C.: R: A language and environment for statistical computing. R Foundation for  
736 Statistical Computing, Vienna, Austria. <https://www.r-project.org/>, 2016.
- 737 Touratier, F., and Goyet, C.: Impact of the Eastern Mediterranean Transient on the distribution of  
738 anthropogenic CO<sub>2</sub> and first estimate of acidification for the Mediterranean Sea, Deep-  
739 Sea Research Part I: Oceanographic Research Papers, 58, 1-15,  
740 10.1016/j.dsr.2010.10.002, 2011.
- 741 Touratier, F., Goyet, C., Houpert, L., de Madron, X. D., Lefèvre, D., Stabholz, M., and  
742 Guglielmi, V.: Role of deep convection on anthropogenic CO<sub>2</sub> sequestration in the Gulf  
743 of Lions (northwestern Mediterranean Sea), Deep-Sea Research Part I: Oceanographic  
744 Research Papers, 113, 33-48, 10.1016/j.dsr.2016.04.003, 2016.
- 745 Turk, D., Malačić, V., DeGrandpre, M. D., and McGillis, W. R.: Carbon dioxide variability and  
746 air-sea fluxes in the northern Adriatic Sea, J. Geophys. Res., 115, C10043,  
747 10.1029/2009JC006034, 2010.
- 748 Vargas, C. A., Contreras, P. Y., Pérez, C. A., Sobarzo, M., Saldías, G. S., and Salisbury, J.:  
749 Influences of riverine and upwelling waters on the coastal carbonate system off Central  
750 Chile and their ocean acidification implications, Journal of Geophysical Research:  
751 Biogeosciences, 121, 1468-1483, 10.1002/2015JG003213, 2016.
- 752 Wootton, J. T., Pfister, C. A., and Forester, J. D.: Dynamic patterns and ecological impacts of  
753 declining ocean pH in a high-resolution multi-year dataset, Proc. Natl. Acad. Sci., 105,  
754 18848-18853, 2008.
- 755 Wootton, J. T., and Pfister, C. A.: Carbon system measurements and potential climatic drivers at  
756 a site of rapidly declining ocean pH, PLoS One, 7, e53396, 2012.
- 757



758 **Table 1.** Ocean acidification studies estimating or documenting pH change in the Mediterranean  
 759 Sea. TrOCA is the ‘Tracer combining Oxygen, inorganic Carbon, and total Alkalinity’ method,  
 760 N.R. means ‘not reported’, and PI is ‘pre-industrial era’. \*indicates studies where the reported  
 761 pH change was assumed to be at *in situ* temperatures.

Region	Site	Method	Study period	pH scale	°C	$\Delta\text{pH yr}^{-1} \pm \text{SE}$	Total $\Delta\text{pH}$	Reference
NW	Point B	time-series, anomaly	2007-2015	total	<i>in situ</i>	$-0.0028 \pm 0.0003$	-0.0252	This study
NW	Point B	time-series, anomaly	2007-2015	total	25	$-0.0017 \pm 0.0002$	-0.0153	This study
NW	Point B	model	1967-2003	total	<i>in situ</i>	-0.0014	-0.05	Howes et al. (2015)
NW	DYFAMED	time-series, observed	1995-2011	seawater	17.34	$-0.003 \pm 0.001$	-0.051	Marcellin Yao et al. (2016)
NW	DYFAMED	time-series comparison	1998-2000, 2003-2005	seawater	<i>in situ</i> *	-	-0.02	Meier et al. (2014)
NW	Gulf of Lion	TrOCA	PI-2011	NR	<i>in situ</i> *	-	-0.15 to -0.11	Touratier et al. (2016)
East	N Adriatic Sea	cruise comparison	1983, 2008	total	25	-0.0025	-0.063	Luchetta et al. (2010)
East	Otranto Strait	TrOCA	PI-1995	seawater	25	-	< -0.1 to -0.05, $\pm 0.014$	Krasakopoulou et al. (2011)
Total	Full profile	TrOCA	PI-2001	NR	<i>in situ</i> *	-	-0.14 to -0.05	Touratier and Goyet (2011)
Total	Bottom waters	model	1800-2001	total	<i>in situ</i> *	-	-0.06 to -0.005	Palmiéri et al. (2015)
Total	Surface waters	model	1800-2001	total	<i>in situ</i> *	-	$-0.084 \pm 0.001$	Palmiéri et al. (2015)
Gibraltar Strait	Espartel sill	pH, pCO <sub>2</sub> sensors	2012-2015	total	25	$-0.0044 \pm 0.00006$	-	Flecha et al. (2015)

762

763



764 **Table 2.** Time-series (observed values and anomalies) regression analyses on seawater carbonate  
 765 chemistry, at Point B, 1 m, for salinity (S), temperature (T, °C), dissolved inorganic carbon ( $C_T$ ,  
 766  $\mu\text{mol kg}^{-1}$ ), total alkalinity ( $A_T$ ,  $\mu\text{mol kg}^{-1}$ ),  $\text{pH}_T$ , 25 °C-normalized  $\text{pH}_T$  ( $\text{pH}_{T25}$ ), calcite ( $\Omega_c$ ) and  
 767 aragonite ( $\Omega_a$ ) saturation state, and salinity-normalized  $A_T$  ( $nA_T$ ) and  $C_T$  ( $nC_T$ ). Slope is change  
 768  $\text{yr}^{-1}$ .  $P \ll 0.001$  indicate p-values far smaller than 0.001.

	<i>Variable</i>	<i>Slope</i> ± <i>SE</i>	<i>Intercept</i> ± <i>SE</i>	<i>F</i>	<i>df</i>	<i>Slope P</i>	<i>R</i> <sup>2</sup>
<b>Observed</b>	S	0.0031 ± 0.0054	31.7 ± 10.8	0.326	1,415	0.568	0.001
	T	0.12 ± 0.08	-226 ± 157	2.429	1,411	0.12	0.006
	$C_T$	2.71 ± 0.31	-3208 ± 626	75.671	1,414	<<0.001	0.155
	$A_T$	2.24 ± 0.21	-1945 ± 418	115.895	1,415	<<0.001	0.218
	$\text{pH}_T$	-0.0031 ± 0.0009	14.3 ± 1.8	11.674	1,410	0.001	0.028
	$\text{pH}_{T25}$	-0.0012 ± 0.0004	10.5 ± 0.9	6.861	1,410	0.009	0.016
	$\text{pCO}_2$	3.78 ± 0.98	-7214 ± 1976	14.82	1,410	<<0.001	0.035
	$\Omega_c$	-0.0043 ± 0.0052	13.9 ± 10.5	0.684	1,410	0.409	0.002
	$\Omega_a$	-0.0017 ± 0.004	6.74 ± 7.98	0.177	1,410	0.674	0
	$nA_T$	2.01 ± 0.31	-1489 ± 632	41.067	1,410	<<0.001	0.091
	$nC_T$	2.57 ± 0.47	-2918 ± 944	29.927	1,410	<<0.001	0.068
	<b>Anomaly</b>	S	-0.0017 ± 0.0044	3.38 ± 8.82	0.147	1,415	0.702
T		0.072 ± 0.022	-145 ± 44	10.999	1,411	0.001	0.026
$C_T$		2.97 ± 0.20	-5965 ± 400	221.87	1,414	<<0.001	0.349
$A_T$		2.08 ± 0.19	-4189 ± 379	122.429	1,415	<<0.001	0.228
$\text{pH}_T$		-0.0028 ± 0.0003	5.72 ± 0.66	74.205	1,410	<<0.001	0.153
$\text{pH}_{T25}$		-0.0017 ± 0.0002	3.46 ± 0.43	64.204	1, 410	<<0.001	0.1354
$\text{pCO}_2$		3.53 ± 0.39	-7105 ± 776	83.927	1,410	<<0.001	0.17
$\Omega_c$		-0.0109 ± 0.0022	22.0 ± 4.5	24.08	1,410	<<0.001	0.055
$\Omega_a$		-0.0064 ± 0.0015	12.9 ± 3.1	17.33	1,410	<<0.001	0.041
$nA_T$		2.20 ± 0.28	-4425 ± 560	62.34	1,410	<<0.001	0.132
$nC_T$		3.12 ± 0.29	-6275 ± 579	117.486	1,410	<<0.001	0.223

769

770



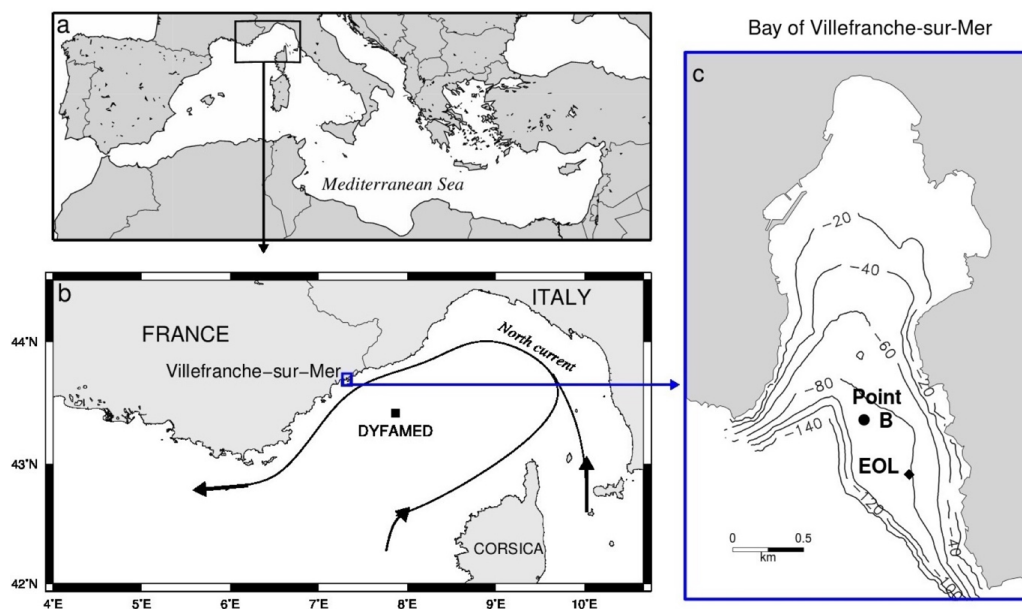
771 **Table 3.** Contribution of temperature ( $T$ ), salinity ( $S$ ), total alkalinity ( $A_T$ ), and dissolved  
 772 inorganic carbon ( $C_T$ ) to observed changes in  $\text{pH}_T$  and  $\text{pCO}_2$  ( $\mu\text{atm}$ )  $\text{yr}^{-1}$ . The sum of the slopes  
 773 ( $\frac{d\text{pH}_T}{dt}$ ,  $\frac{d\text{pCO}_2}{dt}$ ) is slightly inflated compared to the observed trends reported in Table 2 (-0.0037 vs. -  
 774 0.0031  $\text{yr}^{-1}$  for  $\text{pH}_T$ , and 4.26 vs. 3.78  $\mu\text{atm yr}^{-1}$  for  $\text{pCO}_2$ ). These differences are negligible  
 775 relative to the error associated with the slope estimates. Incomplete sum of % contributions are  
 776 due to rounding.  $P$  of  $\ll 0.001$  indicate p-values far smaller than 0.001.

	<i>Variable</i>	<i>Slope ± SE</i>	<i>% contribution</i>	<i>Slope P</i>
	$T$	$-0.0013 \pm 0.0009$	35	0.15
$\frac{\partial \text{pH}_T}{\partial \text{var}} \frac{d\text{var}}{dt}$	$S$	$-0.0002 \pm 0.0008$	5	0.793
	$A_T$	$0.0028 \pm 0.0009$	-76	0.002
	$C_T$	$-0.0050 \pm 0.0009$	135	$\ll 0.001$
$\frac{d\text{pH}_T}{dt}$		-0.0037	99	
	$T$	$1.43 \pm 0.97$	34	0.143
$\frac{\partial \text{pCO}_2}{\partial \text{var}} \frac{d\text{var}}{dt}$	$S$	$0.24 \pm 0.89$	6	0.792
	$A_T$	$-2.94 \pm 0.94$	-69	0.002
	$C_T$	$5.53 \pm 0.96$	130	$\ll 0.001$
$\frac{d\text{pCO}_2}{dt}$		4.26	101	

777



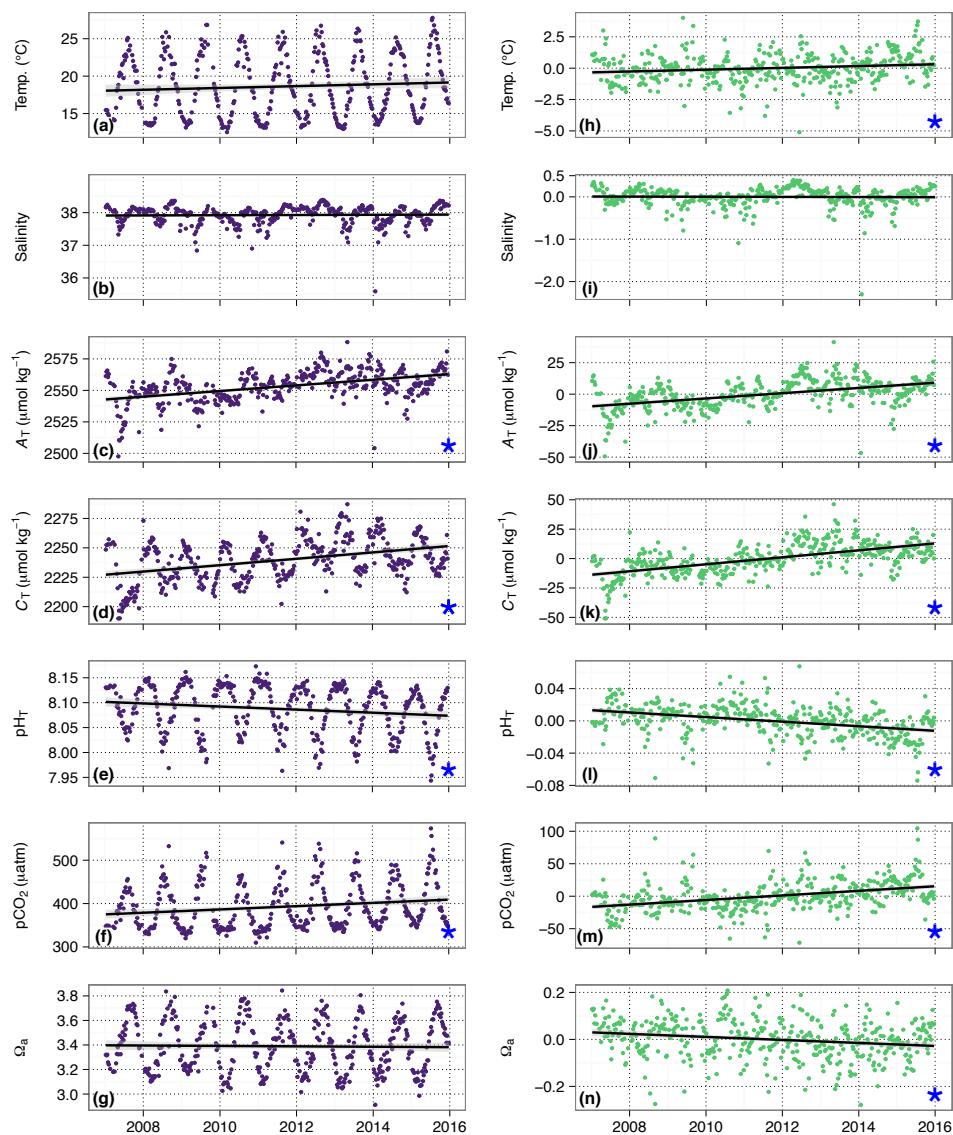
778 **Figure 1.** Map of study region in the NW Mediterranean Sea (a) along the North current (b) in  
779 the Bay of Villefranche-sur-Mer, France (c). Point B station, EOL buoy, and offshore time-series  
780 station DYFAMED are marked. Bathymetric line units are m (c).



781



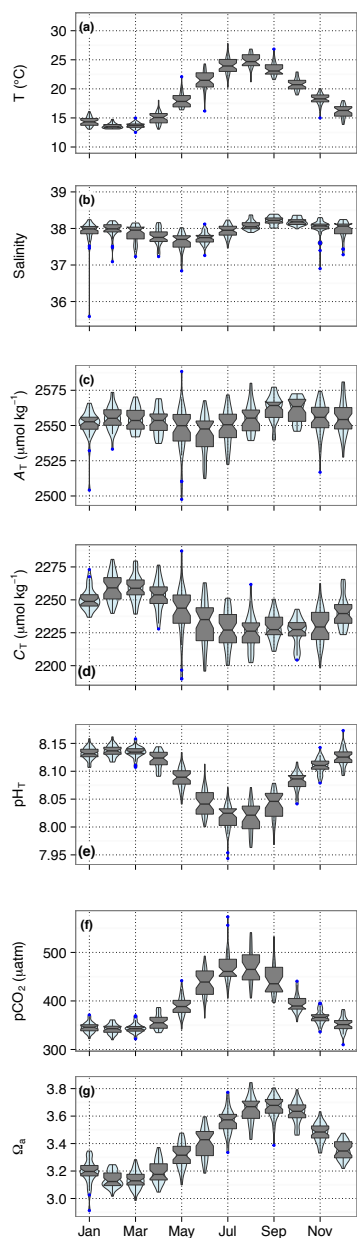
782 **Figure 2.** Time-series observations (a-g) and anomalies (h-n) of temperature, salinity, and  
783 seawater carbonate chemistry at Point B, 1 m. Regression slopes are drawn  $\pm$  SE (in grey) and  
784 noted with a star for significance at  $\alpha=0.05$ .



785



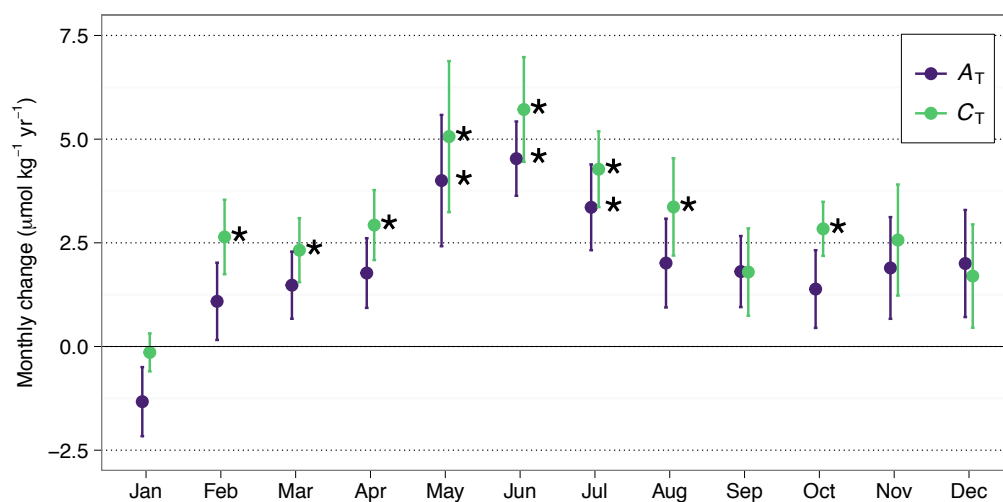
786 **Figure 3.** Monthly distribution of seawater carbonate chemistry at Point B, 1 m., using a  
787 combination of a violin plot showing the relative frequency of the observations (shaded blue  
788 area) and a boxplot showing the median, first and third quartiles, as well as outliers (blue).



789



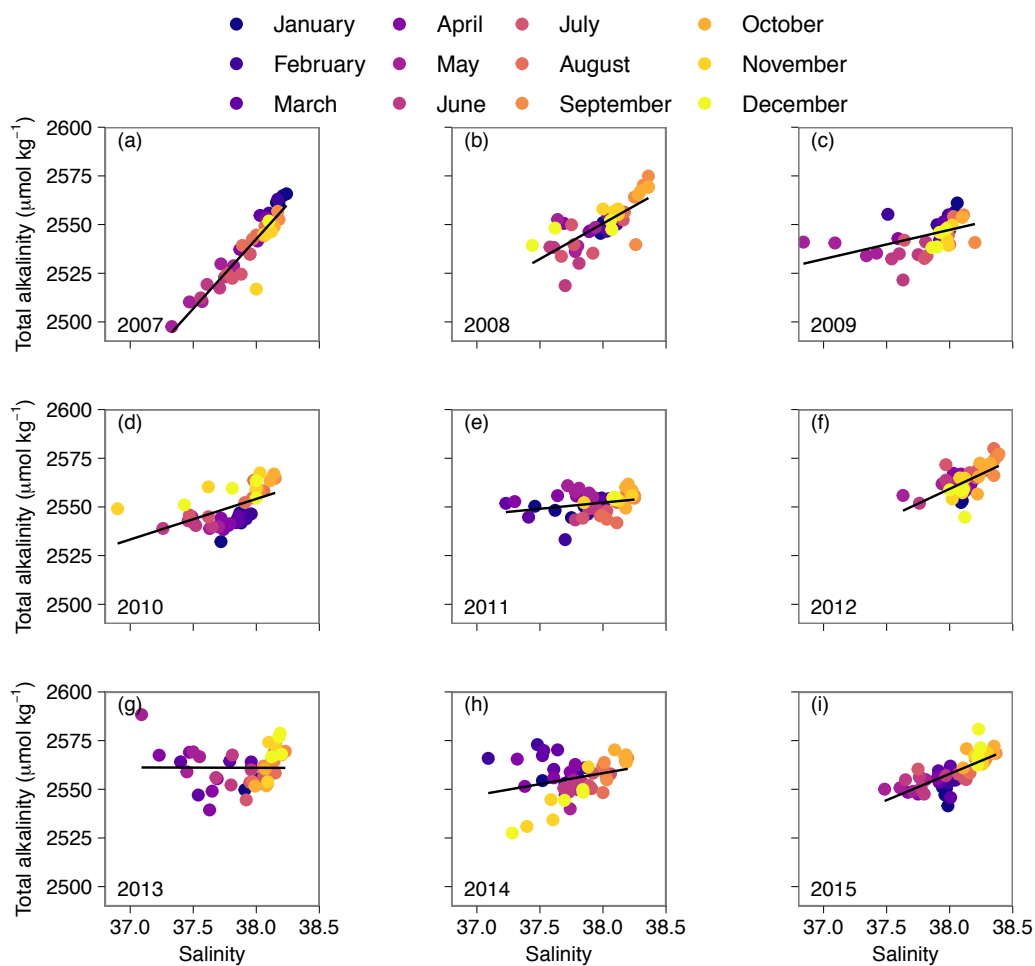
790 **Figure 4.** Increase in total alkalinity ( $A_T$ , purple) and dissolved inorganic carbon ( $C_T$ , green) by  
791 month for the period 2007-2015. Errors bars are  $\pm$  SE of the slope estimate and significance is  
792 noted (\*) at  $\alpha=0.05$ .



793



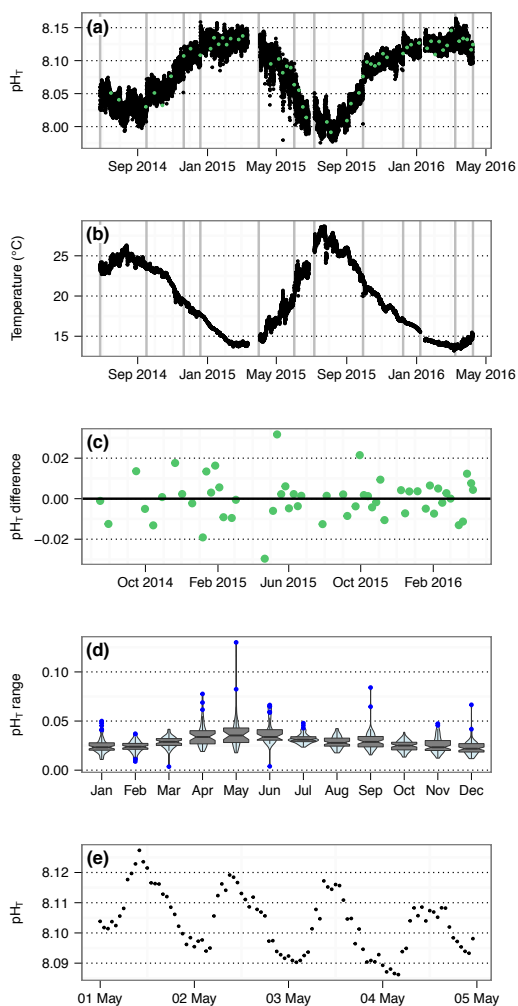
794 **Figure 5.** Salinity and total alkalinity relationships by year for the period 2007-2015, at Point B,  
795 1 m. Data points are colored for month.



796



797 **Figure 6.** Time-series pH (a) and temperature (b) from autonomous SeaFET pH sensor at EOL  
798 buoy, 2 m. Discrete calibration samples are noted in green, and grey vertical lines bracket  
799 deployment periods (a). Mean offset of calibration samples from processed pH time-series was  
800  $\text{pH}_T \pm 0.007$  (c). Diel pH range was small and peaked in April and May (d) and exhibits a clear,  
801 small, diel cycle (e, representative example from May 2015).



802